Chemical Physics Letters 568–569 (2013) 14–20

Contents lists available at SciVerse ScienceDirect

Chemical Physics Letters

journal homepage: www.elsevier.com/locate/cplett

Accurate bond dissociation energy of water determined by triple-resonance vibrational spectroscopy and *ab initio* calculations

Oleg V. Boyarkin [a], Maxim A. Koshelev [a,b], Oleg Aseev [a], Pavel Maksyutenko [a], Thomas R. Rizzo [a], Nikolay F. Zobov [b], Lorenzo Lodi [c], Jonathan Tennyson [c,*], Oleg L. Polyansky [b,c]

[a] *Laboratoire de Chimie Physique Moléculaire, École Polytechnique Fédérale de Lausanne, CH-1015 Lausanne, Switzerland*
[b] *Institute of Applied Physics, Russian Academy of Sciences, Uljanov Street 46, Nizhnii Novgorod 603950, Russia*
[c] *Department of Physics and Astronomy, University College London, London WC1E 6BT, United Kingdom*

ARTICLE INFO

Article history:
Available online 21 March 2013

ABSTRACT

Triple-resonance vibrational spectroscopy is used to determine the lowest dissociation energy, D_0, for the water isotopologue $HD^{16}O$ as 41 239.7 ± 0.2 cm^{-1} and to improve D_0 for $H_2{}^{16}O$ to 41 145.92 ± 0.12 cm^{-1}. *Ab initio* calculations including systematic basis set and electron correlation convergence studies, relativistic and Lamb shift effects as well as corrections beyond the Born–Oppenheimer approximation, agree with the measured values to 1 and 2 cm^{-1} respectively. The improved treatment of high-order correlation terms is key to this high theoretical accuracy. Predicted values for D_0 for the other five major water isotopologues are expected to be correct within 1 cm^{-1}.

1. Introduction

The OH bond dissociation energy of water isotopologues is used in a myriad of applications, ranging from astronomy and biology to combustion and atmospheric chemistry. While extreme accuracy in bond dissociation energies is not typically needed in practical applications, with only three nuclei and 10 electrons, water serves as a benchmark molecule for testing quantum–mechanical calculations. Experimentally, it is a challenge to measure the dissociation energy of even a small polyatomic molecule accurately, as it usually requires access to highly lying molecular levels around D_0 with precisely known energy in a collision-free environment. Theoretically, accurate computations must be performed using extremely sophisticated models with large basis sets and accounting for many effects and interactions that are routinely ignored.

So far, the only highly accurate, sub-cm^{-1} calculations of D_0 validated by accurate experimental data have been for diatomic hydrogen isotopologues [1–3] and their cations [4]. For the simplest polyatomic molecule, H_3^+, D_0 has been calculated to a reported accuracy of 1 cm^{-1} [5] but experimentally confirmed to only about 60 cm^{-1} [6]. The simplicity of these systems means that they do not provide validated theoretical approaches for predicting D_0 of more complex species. Here we report sub-cm^{-1} accuracy measurements of D_0 for $HD^{16}O$, an improved D_0 for $H_2^{16}O$, and *ab initio* calculations of D_0 with an unprecedented accuracy of a few cm^{-1} for seven isotopologues of this molecule.

2. Experimental setup

Several spectroscopic techniques have been employed to improve the accuracy of D_0 for $H_2{}^{16}O$ [7–9]. These experiments converged to an accurate value of $D_0 = 41\,145.94 \pm 0.15$ cm^{-1}, measured by direct observation of the H–OH dissociation continuum by detecting the appearance of OH as a function of the total excitation energy of the water molecule [9]. Here we report a complementary measurement of $D_0(H_2O)$ using triple-resonance vibrational overtone excitation, but by detecting H-atom fragments. This removes any uncertainty that the detected ground state OH may result from hypothetically ultrafast collisional relaxation of the OH fragments, initially appearing in the *f* component of the ground state Λ-doublet, which is slightly higher in energy than the ground state. If this were the case, the measured D_0 would be overestimated by the 0.06 cm^{-1} difference [10] between the two Λ-doublet components. We then employ state-selective overtone excitation to access the dissociation continuum of $H^{16}OD$ on its electronic ground surface to measure D_0 for the OH bond in HOD.

The details of our approach and of the experimental apparatus have been reported elsewhere [9,11–13]; the excitation scheme is illustrated in Figure 1. We use three laser pulses (P1–P3) to access high-lying terminal vibrational levels through sequential excitation of three vibrational overtone transitions. For molecules in terminal levels lying below the dissociation threshold, a second photon of the third excitation laser (P3a) is required to promote them to the repulsive electronic surface. A subsequent laser pulse (P4) detects the appearing photofragments via laser-induced fluorescence. Manipulations with relative polarizations of laser beams

---

* Corresponding author.
E-mail addresses: oleg.boiarkin@epfl.ch (O.V. Boyarkin), j.tennyson@ucl.ac.uk (J. Tennyson).

0009-2614/$ - see front matter
http://dx.doi.org/10.1016/j.cplett.2013.03.007

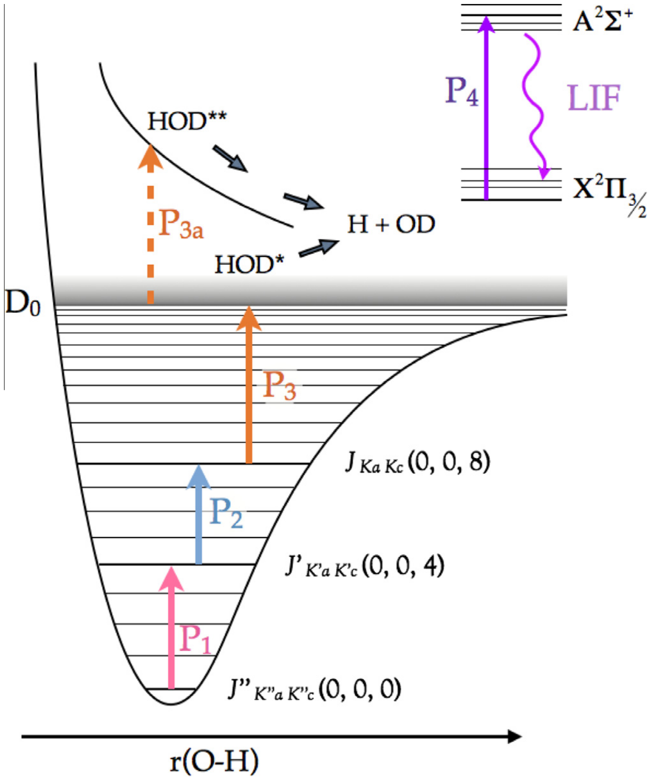

Figure 1. (Color online) Schematic energy level diagram of the triple-resonance scheme for excitation of the OH stretch in HDO with subsequent laser-induced fluorescence (LIF) detection of OD fragments. Molecules in long-lived or bound states near the dissociation threshold D_0 may absorb an additional photon (P3a) from the third excitation laser with subsequent dissociation in the repulsive electronically-excited state.

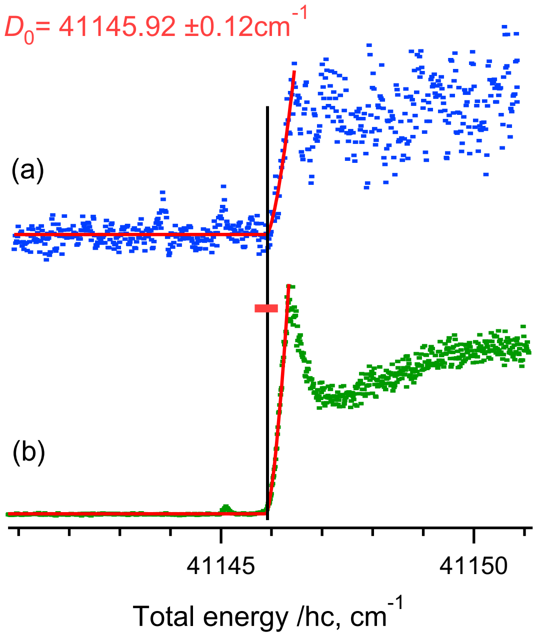

Figure 2. (Color online). Photofragment spectra of H_2O transitions from the gateway state, prepared by the same double resonance transition [27 561.27 cm^{-1} $(9,0)^{+}0,1_{01}] \leftarrow [(4,0)^{-}0,\ 0_{00}]n[(0,0)0,1_{01}]$, to the states with quantum numbers $J = 1$ and 2; and fits of the continuum onsets by the Wigner threshold law with $J = 1$. The spectra are measured at water vapor pressure of 50 μbar by detecting (a) ground state H-atoms, (b) OH in its $[X^2\Pi_{3/2},\ e,\ J = 3/2, v = 0]$ ground state [13]. Both are plotted as a function of the total rovibrational energy.

allow us to control the rotational quantum numbers J of the accessible terminal states using the rotational selection rules.

Figure 2 compares a photodissociation spectrum originating from the $(9,0)^{+}0\ 1_{01}$ gateway state of H_2O, measured by detecting H-atoms (Figure 2a), with the spectrum originating from the same gateway state but measured by detecting ground state OH fragments [12] (Figure 2b). Because of the orthogonal polarizations of P2 and P3, only $J = 1$ and 2 terminal states can be accessed in these measurements. The energy of the onset of the dissociative continuum corresponds to the lowest dissociation energy of the OH bond in the electronic ground state of $H_2{}^{16}O$ through the expression:

$$D_0 = E_0 + h\nu_1 + h\nu_2 + h\nu_3^c \tag{1}$$

where E_0 is the rotational energy of the initial level of H_2O, $h\nu_1$ and $h\nu_2$ are the photon energies of P1 and P2, and $h\nu_3{}^c$ is the energy of photon P3 at the observed onset of the continuum. This expression assumes that the OH fragments are detected in their ground state. Energies of the low-lying vibration–rotation states of both $H_2{}^{16}O$ and $HD^{16}O$ are known very accurately [14–16] and the energies of photons P1–P3 are measured to better than 0.02 cm^{-1}. This leaves most of the uncertainty in determining D_0 on the sharpness of the observed onsets of the dissociative continua. For accurate determination of these onsets we apply the Wigner threshold law [17], fitting both traces in Figure 2 by the function:

$$S(E) = y_0 + a(E - D_0)^{J+1/2} \tag{2}$$

where S is the observed LIF signal, y_0, a and D_0 are the fit parameters, and J is the total angular momentum of the dissociating molecule. For both traces the fits with $J = 1$ and 2 yield very close values of D_0, although those with $J = 1$ are slightly more accurate. Taking together all the fits for $J = 1$ and 2, the 0.06 cm^{-1} linewidth of the P3 laser and the precision of our wavemeter, we come to a value of $D_0(H–OH) = 41\,145.92 \pm 0.12$ cm^{-1} (95% confidence level), which confirms the original result measured by triple resonance [9], which had a greater uncertainty of ±0.15 cm^{-1}.

Figure 3 shows a series of $HD^{16}O$ spectra measured by scanning the third excitation laser (P3) in the region of the continuum onset and plotted as a function of the total internal energy. Although the spectra originate from different rotational and vibrational gateway states, they all exhibit the same onset of the dissociation continuum. Fitting the traces in Figure 3 using the function of Eq. (2) with values of J allowed by the selection rules of the laser pumping scheme yields a set of D_0 values with a standard deviation of ±0.07 cm^{-1} about their average. We excluded from consideration the fit of trace (a) for $J = 0$, because it does not resemble the experimental trace; it is likely that in this case the shape of the onset is largely determined by the transition to the $J = 2$, rather than the $J = 0$, final state. We determine $D_0(H–{}^{16}OD) = 41\,239.7 \pm 0.2$ cm^{-1} within a 95% confidence level. This number is significantly smaller and 25 times more accurate than the recently reported indirect measurement of $41\,283 \pm 5$ cm^{-1} [18]. Our experimental value is strongly supported by the *ab initio* calculations reported below. We rule out any possible artifacts that could have decreased our measured value and thus conclude that the indirect measurements [18] are too high.

3. *Ab initio* calculations

Electronic structure calculations used MOLPRO [19], CFOUR [20] and MRCC [21]. We used basis sets of the Dunning family, aug-cc-p (wC) VnZ (-DK) for n up to 8 [22–26]. The aug-cc-pV7Z and aug-cc-pV8Z basis sets for hydrogen and oxygen were provided privately by Feller, but we had to drop k and l functions as these

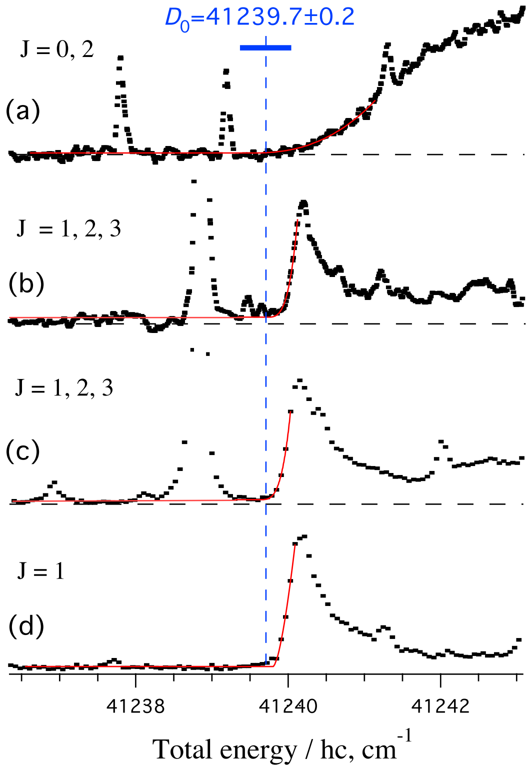

Figure 3. (Color online). Sample photofragment spectra of HD^{16}O transitions (black dots) from the gateway states prepared by the double resonance transition indicated (in normal mode vibrational notation): (a) [27984.79 cm^{-1} (0,0,9),1_{01}] ← [(0,0,4),0_{00}] ← [(0,0,0),1_{01}], (b) [28013.13 cm^{-1} (0,0,9),2_{02}] ← [(0,0,4), 1_{01}] ← [(0,0,0),2_{02}], (c) [25376.10 cm^{-1} (0,0,8),2_{02}] ← [(0,0,4),1_{01}] ← [(0,0,0), 2_{02}], (d) [25376.10 cm^{-1}(0,0,8),0_{00}] ← [(0,0,4),1_{01}] ← [(0,0,0),0_{00}]; and fits of the continuum onsets (red lines) by the Wigner threshold law with J = 2, 3, 3, 1 for (a)–(d) respectively. The spectra are measured by detecting the ground state OD fragments and labeled by the accessible angular momentum quantum numbers. Large peaks of the traces (b) and (c) go beyond the vertical scale. In (a)–(c) the fits ignore the large absorption peaks below the onset for an appropriate fit of the baseline.

are not supported by MOLPRO. We use the shorthand a*n*z to refer to the aug-cc-p*n*VZ basis set, while a[*nm*]z indicates results obtained by extrapolation of the a*n*z and a*m*z values.

For all water isotopologues we used $r_e = 1.8100\ a_0$, $\theta_e = 104.485°$, which are the best mass-independent equilibrium values reported by Császár et al. [27]. For OH we used $r_e = 1.8313\ a_0$, which was obtained by minimization of the energy using IC-MRCI+P (internally-contracted multi-reference configuration interaction with Pople correction, as implemented in MOLPRO), the aug-cc-pwC5Z-DK basis set [26] and the fourth-order Douglas–Kroll–Hess scalar-relativistic Hamiltonian [28].

3.1. Frozen-core CCSD(T) value of D_e

For calculations of the OH radical we used RHF-RCCSD(T), as implemented in MOLPRO. We extrapolated energies using two-point extrapolation and assuming a dependence of the type $E_n = E_\infty + A/n^\alpha$; an analysis of the frozen-core CCSD(T) energies for $n = 3$–6 shows the best fit is obtained for $\alpha = 4$, and this value was therefore used instead of the more traditional value [29] $\alpha = 3$. In agreement with Harding et al. [30] and Feller et al. [29] we did not find any advantage in extrapolating separately the Hartree–Fock and correlation energies when using basis sets larger than 4-ζ. Our best frozen-core value is obtained by extrapolation of the 7-ζ and 8-ζ basis sets and is 43956(6) cm^{-1}, where the error bar is the difference between the a[78]z and non-extrapolated a8z value (see Table 1).

3.2. Use F12 methods

Explicitly correlated methods of the F12 kind [31] were considered but we came to the conclusion that presently-available versions are not adequate at the level of precision of better than 10 cm^{-1} we are aiming for. This conclusion was also recently reached by Patkowski [32], while Feller [33] raised similar concerns. There are a number reasons why presently-available F12 are not adequate for very high accuracies. All F12 versions of the CCSD method (CCSD-F12a, CCSD-F12b, CCSD[F12], CCSD (F12*), etc.) introduce approximations which do not give the same energy as conventional CCSD in the infinite basis set limit. F12 methods require several auxiliary basis sets and the available ones are not large enough for high-accuracy work. There is no F12 version of the (T) correction.

The best value we obtained using an F12 methods is D_e = 43988(8) cm^{-1}, obtained using CCSD(T)-F12b/aug-cc-pV[56]Z. Extrapolation was performed on the D_e values using an exponential, exp ($-an$), law. The uncertainty bar was computed from the combined scatter of a6z and a[56]z values and from the corresponding F12a values. The difference between conventional and F12 values is 32(10) cm^{-1} and hence the two values are incompatible. On the basis of the above discussion we trust the conventional value.

3.3. Core-correlation correction

All-electron calculations used the aug-cc-pwC*n*Z basis sets for $n = 3$–5, and aug-cc-pCV6Z for $n = 6$, as there is no corresponding wC available. We took as core correlation correction the value +80.7(2) cm^{-1}, corresponding to the extrapolated a[56]z CCSD(T) value. The uncertainty bar is the difference between the a6z value and the a[56]z value (see Table 1).

3.4. Higher-level correlation (HLC) effects

We corrected for correlation effects beyond CCSD(T) using CCSDTQ and FCI calculations (see Table 1). There is strong evidence [8,34] that correlation effects due to coupled-cluster quadruple excitations cannot be quantitatively modeled using the 2-ζ basis set, and our study confirms this observation: the RHF–UCCSDTQ – RHF-RCCSD(T) correction is +25.7 cm^{-1} in the cc-pVDZ basis set but −54.9 cm^{-1} in the aug-cc-pVTZ one. Nonetheless 2-ζ results should be representative of the order of magnitude of quadruples. The RHF–UCCSDTQ/aug-cc-pVTZ calculation used the program MRCC [21] and took 38 h and 350 GB of RAM using a single core of a 2.67 GHz Intel Xeon X7542 workstation (the calculation was done fully in RAM to avoid slowdowns due to hard disk input/output). As one can see from Table 1, the small effect due to excitations higher than quadruples shows little basis-set dependence. Even using the extremely small 'single-ζ' 6–31G basis set the FCI-CCSDTQ effect on D_e, namely +1.5 cm^{-1}, is qualitatively similar to the value for the correction obtained in our largest basis set, namely +2.9 cm^{-1}; this basis set is a mixed 2-ζ/3-ζ consisting of cc-pVDZ for hydrogen and cc-pVTZ for oxygen. This FCI calculation took about 5.5 CPU-days, 400 GB of disk and 26 GB RAM. We could not compute FCI/ cc-pVTZ as we estimate such calculation would take about 180 CPU-days, 300 GB of RAM and 7.0 TB of disk. We used for our HLC correction the sum of the RHF–UCCSDTQ/aug-cc-pVTZ correction and of the FCI correction computed in the mixed 2-ζ/3-ζ basis set, namely −54.9 + 2.9 = −52(3) cm^{-1}, where the uncertainty bar takes into account the residual basis-set dependence of HLC at the 3-ζ level.

Note that as both Ruscic et al. [8] and Harding et al. [30] used UHF-based methods their D_e values for the CCSD(T) and the HLC

Table 1
Convergence of non-relativistic electronic contributions to D_e as a function of basis set and model. Electronic energies are in Hartree; D_e values are given in cm^{-1}.

Basis set	Absolute energies in hartrees							D_0 in cm^{-1}		
	Water			OH			H			
	RHF	CCSD	CCSD(T)	RHF	RCCSD	RCCSD(T)	RHF	RHF	CCSD	CCSD(T)
	Frozen core calculations									
a3z	−76.0605709	−76.3336683	−76.3422988	−75.4166792	−75.6394080	−75.6453823	−0.4998212	31,619.8	42,674.4	43,257.4
a4z	−76.0659553	−76.3542109	−76.3635851	−75.4216112	−75.6577103	−75.6642877	−0.4999483	31,691.2	43,138.2	43,752.1
a5z	−76.0672745	−76.3606435	−76.3702976	−75.4228539	−75.6635990	−75.6704112	−0.4999948	31,697.8	43,247.4	43,871.1
a6z	−76.0674164	−76.3628079	−76.3725581	−75.4229835	−75.6655766	−75.6724694	−0.4999993	31,699.5	43,287.4	43,914.6
[56]	−76.0675485	−76.3648240	−76.3746636	−75.4231041	−75.6674187	−75.6743865	−0.5000035	31,701.1	43,324.7	43,955.0
a7z[a]	−76.0674344	−76.3636155	−76.3734052	−75.4229996	−75.6662655	−75.6731891	−0.4999997	31,699.8	43,313.4	43,942.4
a8z[b]	−76.0674408	−76.3639323	−76.3737373	−75.4230040	−75.6665523	−75.6734885	−0.5000000	31,700.2	43,319.9	43,949.5
[78]	−76.0674467	−76.3642274	−76.3740466	−75.4230080	−75.6668194	−75.6737673	−0.5000002	31,700.6	43,326.0	43,956.2
	All-electron calculations							Contribution to D_0		
acw3z	−76.0607273	−76.3905024	−76.3998270	−75.4167902	−75.6960863	−75.7026782	−0.4998212	10.0	34.2	51.0
acw4z	−76.0660122	−76.4148142	−76.4247602	−75.4216501	−75.7180797	−75.7251790	−0.4999483	4.0	51.3	62.3
acw5z	−76.0672871	−76.4221405	−76.4322905	−75.4228628	−75.7247916	−75.7320556	−0.4999948	0.8	66.8	76.5
ac6z	−76.0674204	−76.4247103	−76.4349269	−75.4229863	−75.7271606	−75.7344797	−0.4999993	0.3	69.9	78.7
[56]	−76.0675445	−76.4271040	−76.4373826	−75.4231014	−75.7293671	−75.7367377	−0.5000035	−0.3	72.8	80.7
	CCSD(T)	CCSDTQ	FCI	RCCSD(T)	UCCSDTQ	FCI	RHF	CCSD(T)	CCSDTQ–CCSD(T)	FCI–CCSDTQ
	High-order correlation effects (frozen-core calculations)							Contribution to D_0		
6-31G	−76.1194352	−76.1199484	−76.1199598	−75.4616137	−75.4619457	−75.4619502	−0.4982329	35025.6	+39.8	1.5
2z	−76.2410416	−76.2416589	−76.2416768	−75.5591747	−75.5596750	−75.5596817	−0.4992784	40073.5	+25.7	2.5
2z/3z[c]	−76.3169345	−76.3173241	−76.3173455	−75.6303062	−75.6308607	−75.6308691	−0.4992784	41118.5	−36.2	2.9
a2z	−76.2737613	−76.2744501		−75.5838546	−75.5845560		−0.4993343	41825.8	−2.8	
3z	−76.3321941	−76.3325898		−75.6375536	−76.6381265		−0.4998098	42760.4	−38.9	
a3z	−76.3422988	−76.3427192		−75.6453823	−75.6460531		−0.4998212	43257.4	−54.9	

[a] *k* Functions dropped.
[b] *k* and *l* Functions dropped.
[c] cc-pVDZ basis set for hydrogen and cc-pVTZ for oxygen.

are not directly comparable with ours, while their sum, corresponding to the FCI/infinite-ζ limit, is.

3.5. Relativistic and QED corrections

The scalar-relativistic correction was computed using the sixth-order Douglas–Kroll–Hess (DKH) Hamiltonian [28] and the aug-cc-pwC5Z-DK basis set. The dependence both on basis set size (for basis sets larger than 3-ζ) and correlation treatment (various versions of the CCSD(T) method and IC-MRCI+Q were tried) are small, <2 cm^{-1}. Our best value is −53(3) cm^{-1}, obtained with the AQCC method in the full-valence reference space. Values for the relativistic correction obtained using the simple mass-velocity, one-electron Darwin (MVD1) Hamiltonian are systematically 2.9 cm^{-1} smaller than the DKH values.

The order of magnitude of quantum electrodynamic (QED) corrections was estimated as 0.0238 times the one-electron Darwin term [35]. Its value is 3.2 cm^{-1} using MRCI/aug-cc-pwCV5Z. Tests using smaller basis sets and different correlation treatments (CASSCF and ACPF) show that this value is converged to 0.2 cm^{-1}.

3.6. Born–Oppenheimer diagonal correction (BODC)

The BODC was computed using CFOUR [20] at the UHF–CCSD level. Correlation effects further than CCSD are estimated to affect DOBC values by less than 1 cm^{-1} on the basis of the cc-pVDZ/CISDT values for water reported by Valeev and Sherrill [36]. We used the following (nuclear) masses: $m(H) = 1.00727645$ Da, $m(D) = 2.01355320$ Da, $m(^{16}O) = 15.99052599$ Da, $m(^{17}O) = 16.99474256$ Da and $m(^{18}O) = 17.99477166$ Da. We used the aug-cc-pVTZ and aug-cc-pVQZ basis sets and extrapolated the BODC values assuming an n^{-3} dependence. The extrapolated values are reported in Table 3 and are converged with respect to the basis set to 0.2 cm^{-1}. The BODC corrections for the H and D atoms are given in atomic units by $1/(2M)$ and amount to, respectively, 59.8 and 29.9 cm^{-1}.

3.7. Zero-point energies and spin–orbit effect

The zero-point energy of a molecule is usually defined as the difference between the energy of the rotational–vibrational ground state and the energy of the lowest point of the potential energy surface (PES) [37]. Some qualifications necessary in the case of open-shell species are discussed in the section devoted to the OH/OD diatomics.

All water calculations used the DVR3D program suite [38] and nuclear masses. For $H_2{}^{16}O$ we used the recent semi-empirical PES by Bubukina et al. [39] and the *ab initio* CVRQD surface by Barletta et al. [40]. For HDO we tried a semi-empirical PES [41] and the CVRQD surface without the adiabatic correction. The sensitivity to the PES used is less than 0.4 cm^{-1}. Using atomic masses results in ZPE which are smaller by 1.2, 0.6 and 0.5 cm^{-1} for the isotopologues containing respectively two H atoms, one H and one D and two D atoms. For all isotopologues the error bar on ZPEs can be conservatively estimated to 0.5 cm^{-1}.

The water $^1A_1$ ground state is a spin-singlet and the spin–orbit effect is zero at first order of perturbation theory. The second order effect is mostly due to couplings with the excited states $^3B_1$, $^1B_1$ and $^3A_1$ (all lying between 59000 cm^{-1} and 78000 cm^{-1}) and was estimated to be smaller than 0.02 cm^{-1} using IC-MRCI/aug-cc-pVTZ. This estimate holds for all water isotopologues.

The Hamiltonian appropriate for understanding the spectra of diatomic molecules within ≈1–2 cm^{-1} can be written as [42]:

$$\mathbf{H} = -\frac{\hbar^2}{2\mu}\frac{d^2}{dr^2} + V(r) \qquad (3)$$

Table 2
Ab initio contributions to the dissociation energies of $H_2{}^{16}O$ and $HD^{16}O$. All values are in cm^{-1}. Results of the previous *ab initio* studies [8,30] are given for comparison. Uncertainties, where available, are given in parenthesis. Signed contributions are additive corrections. Contributions A to H are nuclear-mass independent, all others are nuclear-mass dependent (MD).

		Ref. [8]	Ref. [30]	This work
A	CCSD(T) frozen core	43957(52)		43956(6)
B	Core correlation CCSD(T)	+77		+81(2)
C	All-electron CCSD(T) [=A + B]	44034	+13424	44037(6)
D	Higher-order correlation	−7	−25	−52(3)
E	Full CI value [=C + D]	44027	44000	43985(7)
	MRCI+Q value			43984(60)
F	Scalar relativistic correction	−53	−50	−53(3)
G	QED (Lamb shift) correction			+3(1)
H	Spin–orbit effect		−65	−69.4(1)
I	Angular momenta coupling, OH			+31.5(0)
J	Sum spin effects, OH [=H + I]	−38	−65	−37.9(1)
K	BODC, H_2O	+36	+35	+35.3(0.5)
L	ZPE H_2O	−4638		−4638.1(0)
M	ZPE OH	+1851		+1850.7(0.5)
N	Net ZPE, H_2O [=L + M]	−2787	−2804	−2787.4(0.5)
O	Angular momenta coupling, OD			+18.1(0)
P	Sum spin effects, OD [=H + O]			−51.3(1)
Q	BODC, HDO			+26.9(0.5)
R	ZPE HDO			−4023.0(0)
S	ZPE OD			+1350.8(0.5)
T	Net ZPE, HDO [=R + S]			−2672.2(0.5)
U	Non-adiabatic contributions			0(1)
V	Total MD, H_2O [=I + K+N + U]			−2721(1)
W	Total MD, HDO [=O + Q+T + U]			−2627(1)
	$D_0(H_2O)$ Calc. [=E + V]	41187(52)	41116	41145(8)
*	(Obs − Calc) $D_0(H_2O)$	−42	+30	+1
	D_0(HDO) Calc. [=E + W]			41238(8)
*	(Obs − Calc) D_0(HDO)			+2
	Δcalc = $D_0(H_2O) - D_0$(HDO) [=V-W]			−93.4(0.9)
	Δobs = $D_0(H_2O) - D_0$(HDO)			−93.8(0.3)
*	Δobs − Δcalc			−0.5

$$+B[J(J+1)+S(S+1)-\Lambda^2-2\Omega^2+2\Lambda\Omega] \tag{4}$$

$$+B[L_x^2(r)+L_y^2(r)] \tag{5}$$

$$+\mathbf{H}^{SO}+\mathbf{H}^{LS}+\mathbf{H}^{JL}+\mathbf{H}^{JS} \tag{6}$$

where all symbols have their usual spectroscopic meaning, $V(r)$ is the adiabatic potential energy curve and the terms (6) represent the spin–orbit, spin-electronic, L-uncoupling and S-uncoupling operators [42]. A detailed analysis shows that for molecules in energetically well-isolated $^1\Sigma$ states all terms given by (4)–(6) are either exactly zero or negligibly small for rotationless ($J = 0$) states. In this simplified case the ZPE can be obtained by solving the one-dimensional Schrödinger equation given by Eq. (3). In the case of open-shell molecules ($S \neq 0$ and/or $\Lambda \neq 0$) terms (4)–(6) cannot be ignored as they significantly contribute to the energy of rotational–vibrational states. This situation notwithstanding, it is common practice to compute ZPEs for open-shell species using the same procedure used for closed-shell species, i.e. by solving Eq. (3). To aid comparison with the existing literature we followed this convention for the ZPEs of all the OH isotopologues. More specifically, we decomposed the energy of the rotational–vibrational ground state of the OH/OD diatomics as E_{tot} = ZPE + E_{SO} + $E_{coupling}$. E_{tot} was obtained by solving the coupled problem (3)–(6), using an in-house program. ZPE is the conventional zero-point energy obtained by solution of (3). E_{SO} is the spin–orbit contribution due to $\mathbf{H}^{SO}$, computed at the electronic-structure step, discussed below. The term $E_{coupling}$ is given by E_{tot} – ZPE – E_{SO} and represents the net contribution due to terms (4)–(6). A similar approach was used by Harding et al. [30], who for the coupled problem used an approximate formula by Hill and van Vleck [43]; note that Ref. [30] calls our E_{SO} + -$E_{coupling}$ 'spin–orbit stabilization energy'. Ruscic [8] too uses the Hill-van Vleck formula and calls E_{SO} + $E_{coupling}$ 'spin orbit contribution' without any further qualification. We prefer to keep the two contributions E_{SO} and $E_{coupling}$ separate as the former is nuclear-mass-independent, while the latter is nuclear-mass-dependent.

To calculate zero point energies we built an *ab initio* potential energy curve (PEC) using all-electron IC-ACPF/DKH4 and the aug-cc-pwC5Z-DK basis set. Nuclear masses were used for all isotopologues. The PEC was built by spline interpolants from 200 equally-spaced points between 1.00 a_0 and 3.00 a_0. We then complemented this PEC with four further small corrections: (a), term (5), proportional to the expectation value of the $L_x^2 + L_y^2$ operator; (b), an electron-correlation correction curve based on seven Full-CI (frozen core) points computed in the cc-pVTZ basis set; (c) a basis-set extrapolation correction surface based on a coarser IC-ACPF/DKH4 curve computed with the aug-cc-pCV6Z basis set; (d), an adiabatic correction curve computed with CCSD/aug-cc-pVDZ. Using this composite surface we obtain an equilibrium bond length r_e = 1.832 a_0 while the ZPE for OH is 1850.73 cm^{-1}. These values agree very well with the experimentally-derived value reported by Irikura [37] ZPE = 1850.69(5) cm^{-1} (based on data from Ref. [44]), also used by Ruscic [8], and r_e = 1.834 a_0 [44]. Harding et al. [30] quote 1850.69 cm^{-1} as the correct experimental value for OH, but in their Table 1 use, for reasons of consistency, the *ab initio* value given by HEAT protocol, namely 1859.9 cm^{-1}. Our *ab initio* PEC was used to predict the ZPE for all the OH isotopologues considered. Results for ZPE, along with the spin–orbit and angular-momentum contributions are reported in Table 3:

The Breit-Pauli spin–orbit Hamiltonian [42] splits the energy of the $^2\Pi$ ground state of the OH diatomic into two components, $^2\Pi_{3/2}$ and $^2\Pi_{1/2}$, with the $^2\Pi_{3/2}$ curve lying lowest. If spin–orbit couplings of the $^2\Pi$ components with further excited states are neglected the shifts of the $^2\Pi_{3/2}$ and $^2\Pi_{1/2}$ components are given by ±(A/2), where $|A|$ represents the separation of the two $^2\Pi$ components. Herzberg and Huber [44] report $A = -139.21$ cm^{-1} while a recent analysis by

Table 3
Predicted bond dissociation energies D_0 for water isotopologues. All quantities in cm^{-1}.

Bond	BODC[a]		ZPE[b]		AMC[c]	MDC[d]	D_0
	H_2O	OH	H_2O	OH			
^{16}OH–H	611.2	586.8	4638.1	1850.7	31.4	−2720.7	41146.0
^{17}OH–H	580.3	555.7	4630.4	1847.5	31.3	−2716.4	41150.3
^{18}OH–H	553.0	528.2	4623.3	1844.6	31.2	−2712.5	41154.2
^{16}OD–H	589.0	556.1	4023.0	1350.8	17.9	−2627.0	41239.7
^{16}OH–D	589.0	586.8	4023.0	1850.7	31.4	−2112.9	41753.8
^{17}OD–H	558.1	525.1	4013.3	1346.4	17.8	−2622.4	41244.3
^{17}OH–D	558.1	555.7	4013.3	1847.5	31.3	−2107.0	41759.7
^{18}OD–H	530.8	497.6	4005.0	1342.4	17.7	−2618.3	41248.4
^{18}OH–D	530.8	528.2	4005.0	1844.6	31.2	−2101.8	41764.9
^{16}OD–D	566.8	556.1	3390.0	1350.8	17.9	−2002.0	41864.7

[a] Born–Oppenheimer diagonal corrections. Contributions due to the H and D atoms are 59.8 and 29.9 cm^{-1}. The overall contributions to D_0 is given by BODC (OH)+BODC (H)-BODC (H_2O).

[b] Zero-point energy contributions. The overall contributions is given by ZPE (OH)-ZPE (H_2O).

[c] Total contribution to D_0 due to angular-momenta coupling in the OH diatomics.

[d] Overall mass-dependent contribution to D_0, given by the sum of the BODC and ZPE total contributions.

Bernath and Colin [10] gives $A = -139.05\ cm^{-1}$. We computed *ab initio* the value of A for $r = 1.835\ a_0$ using IC-MRCI, the aug-cc-pwCnZ-DK basis sets (n = T, Q, 5) and the fourth-order Douglas–Kroll–Hess Hamiltonian. For basis sets of increasing size with n = T, Q, 5 the values −134.2, −137.3 and −138.7 cm^{-1} were obtained. Our final value for the shift of the $^2\Pi_{3/2}$ component (contribution (H) in Table 2) is $A/2 = -69.4(1)\ cm^{-1}$.

The coupled system given by terms (3)–(6) was solved using an in-house program and the potential energy curve and spin–orbit constant A discussed in the previous sections. Coupling with excited electronic terms were neglected. Subtracting from the energies relative to the fully-coupled system the ZPEs and the spin–orbit contribution gives the values reported in Table 3.

3.8. Non-adiabatic effects

Non-adiabatic (NA) effects are notoriously difficult to evaluate; they contribute 0.4339(2) cm^{-1} to the dissociation energy of H_2 and 0.1563(2) cm^{-1} to the dissociation energy of D_2 [3], even though they contribute up to 4.7 cm^{-1} in magnitude for rotational–vibrational energy levels [45]. Schwenke [46] reported non-adiabatic corrections relative to the vibrational ground state down to −1.7 cm^{-1} for water vibrational energy levels up to $\approx$10000 cm^{-1}; the absolute contribution to the ground vibrational state is not reported by [46].

Here we estimate the magnitude of NA effects using a recent adaptation of Schwenke's procedure [47] to be less than 1 cm^{-1} for the overall error bar for D_0.

4. Discussion

Results of our computations are compared with the best previous studies [8,30,48] and detailed in Table 2. Our calculations considered the following contributions to D_0: (A) correlated electronic energy calculated at the coupled cluster CCSD(T) level; (B) a core-correlation correction; (C) [=A + B] a complete basis set, all electron CCSD(T) value; (D) higher-level electron correlation correction (HLC); (E) [=C + D] a complete basis set, full configuration interaction value; (F) an electronic scalar-relativistic correction; (G) QED Lamb-shift correction; (H) an electronic spin–orbit coupling correction; (I, O) contributions due to angular-momenta couplings in the OH or OD radical; (J) [=H + I] and (P) [=H + O] overall spin-related effects in the OH or OD radical; (K, Q) BODC; and (L, M, N, R, S, T) vibrational zero point energy (ZPE) contributions relative to the various isotopologues. Contributions (A) to (H) only concern the electronic motion with fixed nuclei. Contributions (I) to (T) involve solving the nuclear-motion problem for water and for the OH diatomic. (U) NA effects are estimated as zero but with a contribution to D_0 which may conceivably amount to up to 1 cm^{-1}.

The overall accuracy of our theoretical value for D_0 is determined mainly by the basis-set incompleteness error of the main contribution (C), namely valence-only CCSD(T), even though we used very large aug-cc-pV7Z and aug-cc-pV8Z basis sets [29] and basis-set extrapolation. The core-correlation contribution, also included in contribution (C), was computed using extrapolation of the aug-cc-pwC5Z and aug-cc-pC6Z basis sets and carries an uncertainty of 2 cm^{-1}. Our HLC contribution (D) is essential for obtaining good agreement with the measurements and is based on CCSDTQ in the aug-cc-pVTZ basis set and Full CI in a hybrid basis set which uses cc-pVTZ for oxygen and cc-pVDZ for hydrogen. The Full CI correction to the CCSDTQ value amounts to 2.9 cm^{-1} and is consistent with the value given by Feller and Peterson [48] for their correction to the atomization energy of water, namely 3.5 cm^{-1}. Differences with previous values [8,30] for contributions (A) to (D) are partly due to a slightly different partitioning of the CCSD(T) and HLC contributions; however, the full CI estimated value (E) is directly comparable between all references. A significant factor in our HLC contribution (D) is our use of the larger aug-cc-pVTZ basis set instead of the smaller cc-pVDZ (or analogous) basis generally used previously.

The angular momenta coupling contributions (I, O) arise from the $^2\Pi$ electronic ground states of the OH and OD diatomics; the presence of angular momenta (electronic spin and orbital) implies that the minimum total angular momentum J for these systems is 3/2 and leads to small but relevant energy contributions, discussed in the supplemental material. Note that the previous studies [8,30] provide the sum of the contributions (H) and (I) as their 'spin–orbit contribution'.

The ±8 cm^{-1} uncertainty in the calculated dissociation energies, which is smaller than previous values [8,47,48] by a factor of more than five, is largely determined by the mass-independent contribution (E). The isotopic shift of D_0, $\Delta = D_0(H_2O) - D_0(HDO)$, is entirely determined by the mass-dependent (adiabatic and non-adiabatic) contributions and was calculated more accurately than D_0. Comparison of observed and calculated values gives $\Delta(\text{obs}) - \Delta(\text{calc}) = 0.5 \pm 1.2\ cm^{-1}$, indicating once again agreement within the stated uncertainties.

We note that the coupled-cluster approach employed is applicable because we perform separate calculations for the water molecule and for the dissociation fragments (OH, OD and H) at their equilibrium geometry. It is well established, [49] that the truncated coupled-cluster methods such as CCSD(T) perform poorly in the near-dissociation region and that the computation of global potential energy surfaces requires methods such as multi-reference configuration interaction (MRCI) [50]. Table 2 shows that the value for the mass-independent, non-relativistic contribution to D_0 computed with Davidson-corrected MRCI is within 2 cm^{-1} of our coupled-cluster based full-CI estimate. The agreement between the coupled-cluster and the MRCI value opens the way to MRCI-based *ab initio* studies of the entire water ground state potential energy surface both below and above dissociation with an accuracy of only a few cm^{-1}.

Finally our mass-dependent terms can be combined with the measured values for D_0 to provide predicted dissociation energies for the other isotopologues of water, see Table 3. For all isotopologues we use a mass-independent contribution of 43866.7 (1.5) cm^{-1}, obtained by combining the experimental values for $D_0(H_2O)$ and $D_0(HDO)$ and the corresponding theoretical mass-dependent contributions. The less accurate *ab initio* mass-independent contribution is given by the sum of contribution (E), (F), (G) and (H) of Table 2 and is 43865(8) cm^{-1}. Also reported are the zero-point energies (ZPE) and Born–Oppenheimer diagonal correction (BODC) contributions as well as the overall mass-dependent contribution (MDC). We estimate the predicted values of D_0 should be accurate to 1 cm^{-1}.

5. Conclusions

Our measurements improve the earlier value of D_0 for $H_2{}^{16}O$ to 41 145.94 ± 0.12 cm^{-1} and provide a value D_0(H–OD) = 41 239.7 ± 0.2 cm^{-1} for $HD^{16}O$. These two values, currently the most accurate available, enable a double assessment of the accuracy of our high-level *ab initio* computations. Theory reproduces both measured values within ±2 cm^{-1}, that is, with a relative accuracy better than 0.005%. Such highly accurate calculations inspire confidence in the ability of our theoretical approach to predict yet unmeasured molecular quantities at the interface of discrete and continuum quantum states with a similar accuracy. In particular, predicted D_0 values for several isotopologues of water, obtained as a theoretical shift to the measured D_0 values, are given in Table 3 and provide a subject for further experimental verification.

Acknowledgements

This work was supported by Swiss State Secretary for Education and Research (CH-RU STC program), by Swiss National Science Foundation (Grant No. 129649), the European Research Council Advanced Investigator Project 267219 and the Russian Fund for Fundamental Research.

References

[1] J.J. Liu, E.J. Salumbides, U. Hollenstein, J.C.J. Koelemeij, K.S.E. Eikema, W. Ubachs, et al., J. Chem. Phys. 130 (2009) 174306.

[2] D. Sprecher, J.J. Liu, C. Jungen, W. Ubachs, F. Merkt, J. Chem. Phys. 133 (2010) 111102.

[3] K. Piszczatowski, G. Łach, M. Przybytek, J. Komasa, K. Pachucki, B. Jeziorski, J. Chem. Theory Comput. 5 (2009) 3039.

[4] Y.P. Zhang, C.H. Cheng, J.T. Kim, J. Stanojevic, E.E. Eyler, Phys. Rev. Lett. 92 (2004) 203003.

[5] W. Kutzelnigg, R. Jaquet, Philos. Trans. R. Soc. A 364 (2006) 2855.

[6] A. Petrignani et al., Phys. Rev. A 83 (2011) 032711.

[7] S.A. Harich, D.W.H. Hwang, X.F. Yang, J.J. Lin, X.M. Yang, R.N. Dixon, J. Chem. Phys. 113 (2000) 10073.

[8] B. Ruscic, A.F. Wagner, L.B. Harding, R.L. Asher, D. Feller, D.A. Dixon, et al., J. Phys. Chem. A 106 (2002) 2727.

[9] P. Maksyutenko, T.R. Rizzo, O.V. Boyarkin, J. Chem. Phys. 125 (2006) 181101.

[10] P.F. Bernath, R. Colin, J. Mol. Spectrosc. 257 (2009) 23.

[11] P. Maksyutenko, J.S. Muenter, N.F. Zobov, S.V. Shirin, O.L. Polyansky, T.R. Rizzo, et al., J. Chem. Phys. 126 (2007) 241101.

[12] M. Grechko, O.V. Boyarkin, T.R. Rizzo, P. Maksyutenko, N.F. Zobov, S.V. Shirin, et al., J. Chem. Phys. 131 (2009) 221105.

[13] M. Grechko, P. Maksyutenko, T.R. Rizzo, O.V. Boyarkin, J. Chem. Phys. 133 (2010) 81103.

[14] J. Tennyson, N.F. Zobov, R. Williamson, O.L. Polyansky, P.F. Bernath, J. Phys. Chem. Ref. Data 30 (2001) 735.

[15] J. Tennyson et al., J. Quant. Spectrosc. Radiat. Transf. 111 (2010) 2160.

[16] J. Tennyson, P.F. Bernath, L.R. Brown, A. Campargue, M.R. Carleer, A.G. Császár, et al., J. Quant. Spectrosc. Radiat. Transf. 117 (2013) 29.

[17] E.P. Wigner, Phys. Rev. 73 (1948) 1002.

[18] L. Cheng, K. Yuan, Y. Cheng, Q. Guo, T. Wang, D. Dai, et al., J. Phys. Chem. A 115 (2011) 1500.

[19] H.J. Werner, P.J. Knowles, G. Knizia, F.R. Manby, M. Schütz, *WIREs Comput. Mol. Sci* **2** (2012) 242.

[20] CFOUR, 2010. CFOUR, Coupled-Cluster techniques for Computational Chemistry, a quantum-chemical program package by J.F. Stanton, J. Gauss, M.E. Harding, P.G. Szalay with contributions from A.A. Auer, R.J. Bartlett, U. Benedikt, C. Berger, D.E. Bernholdt, Y.J. Bomble, L. Cheng, O. Christiansen, M. Heckert, O. Heun, C. Huber, T.-C. Jagau, D. Jonsson, J. Jusélius, K. Klein, W.J. Lauderdale, D.A. Matthews, T. Metzroth, L.A. Mück, D.P. O'Neill, D.R. Price, E. Prochnow, C. Puzzarini, K. Ruud, F. Schiffmann, W. Schwalbach, S. Stopkowicz, A. Tajti, J. Vzquez, F. Wang, J.D. Watts and the integral packages MOLECULE (J. Almlöf and P.R. Taylor), PROPS (P.R. Taylor), ABACUS (T. Helgaker, H.J. Aa. Jensen, P. Jørgensen and J. Olsen), and ECP routines by A.V. Mitin and C. van Wüllen. For the current version, see http://www.cfour.de.

[21] M. Kállay, P.R. Surján, J. Chem. Phys. 115 (2001) 2945. MRCC, a string-based quantum chemical program suite written by M. Kállay. See http://www.mrcc.hu.

[22] T.H. Dunning, J. Chem. Phys. 90 (1989) 1007.

[23] R. Kendall, T. Dunning, R. Harrison, J. Chem. Phys. 96 (1992) 6796.

[24] A.K. Wilson, T. van Mourik, T. Dunning, J. Mol. Struct. (THEOCHEM) 388 (1997) 339.

[25] K. Peterson, T. Dunning, J. Chem. Phys. 117 (2002) 10548.

[26] W. de Jong, R. Harrison, D. Dixon, J. Chem. Phys. 114 (2001) 48.

[27] A. Császár, G. Czakó, T. Furtenbacher, J. Tennyson, V. Szalay, S. Shirin, et al., J. Chem. Phys. 122 (2005) 214305.

[28] D. Peng, K. Hirao, J. Chem. Phys. 130 (2009) 044102.

[29] D. Feller, K.A. Peterson, J.G. Hill, J. Chem. Phys. 135 (2011) 044102.

[30] M.E. Harding, J. Vazquez, B. Ruscic, A.K. Wilson, J. Gauss, J.F. Stanton, J. Chem. Phys. 128 (2008) 114111.

[31] L. Kong, F.A. Bischoff, E.F. Valeev, Chem. Rev. 112 (2012) 75.

[32] K. Patkowski, J. Chem. Phys. 137 (2012) 034103.

[33] D. Feller, J. Chem. Phys. 138 (2013) 074103.

[34] J. Csontos, M. Kállay, J. Phys. Chem. A 115 (2011) 7765.

[35] P. Pyykkö, K. Dyall, A. Császár, G. Tarczay, O. Polyansky, J. Tennyson, Phys. Rev. A 63 (2001) 024502.

[36] E.F. Valeev, C.D. Sherrill, J. Chem. Phys. 118 (2003) 3921.

[37] K.K. Irikura, J. Phys. Chem. Ref. Data 36 (2007) 389.

[38] J. Tennyson, M.A. Kostin, P. Barletta, G.J. Harris, O.L. Polyansky, J. Ramanlal, et al., Comput. Phys. Commun. 163 (2004) 85.

[39] I. Bubukina, N. Zobov, O. Polyansky, S. Shirin, S. Yurchenko, Opt. Spectrosc. 110 (2011) 160.

[40] P. Barletta, S.V. Shirin, N.F. Zobov, O.L. Polyansky, J. Tennyson, A.G. Császár, J. Chem. Phys. 125 (2006) 204307.

[41] S. Yurchenko et al., J. Chem. Phys. 128 (2008) 044312.

[42] H. Lefebvre-Brion, R.W. Field, The Spectra and Dynamics of Diatomic Molecules, Academic Press, 2004.

[43] E. Hill, J. van Vleck, Phys. Rev. 32 (1928) 250.

[44] K. Huber, G. Herzberg, Molecular Spectra and Molecular Structure IV, Constants of Diatomic Molecules, Reinhold, Van Nostrand, 1979.

[45] Komasa, K. Piszczatowski, G. Łach, M. Przybytek, B. Jeziorski, K. Pachucki, J. Chem. Theory Comput. 7 (2011) 3105.

[46] D.W. Schwenke, J. Phys. Chem. A 105 (2001) 2352.

[47] O.L. Polyansky, R.I. Ovsyannikov, A.A. Kyuberis, L. Lodi, J. Tennyson, N.F. Zobov, J. Phys. Chem. A. (in press). http://dx.doi.org/10.1021/jp312343z.

[48] D. Feller, K.A. Peterson, J. Chem. Phys. 131 (2009) 154306.

[49] D.I. Lyakh, M. Musiał, V.F. Lotrich, R.J. Bartlett, Chem. Rev. 112 (2012) 182.

[50] P.G. Szalay, T. Muller, G. Gidofalvi, H. Lischka, R. Shepard, Chem. Rev. 112 (2012) 108.